9卷2期 地震工程与工程振动 Vol.9, No.2
1989年6月 EARTHQUAKE ENGINEERING AND ENGINEERING VIBRATION June,1989

EMPIRICAL SCALING OF FOURIER SPECTRUM AMPLITUDES OF RECORDED STRONG EARTHQUAKE ACCELERATIONS IN TERMS OF MAGNITUDE AND LOCAL SOIL AND GEOLOGIC CONDITIONS

by

M.D.Trifunac
(University of Southern California, U.S.A.)

ABSTRACT

New scaling equations for Fourier amplituds spectra of strong earthquake accelerations are presented for characterization of local site conditions in terms of soil and geologic site classification parameters. It is shown that both soil and geologic site conditions should be used together in estimation of the site specific spectrum amplitudes.

INTRODUCTION

The influence of local soil or geological site conditions on amplitudes of recorded seismic waves has been investigated theoretically (e. g.Haskell, 1960;Tsai, 1969; Trifunac, 1971) and experimentally (e. g. Kanai, 1949, 1951; Gutenberg, 1957; Duke, 1958; Medvedev, 1955; Zhou, 1965) by considering various overall measures of strong shaking amplitudes. Through comparison of the shapes of the Fourier and response spectrum amplitudes (Zhou,1965), it became possible to describe the average effects the local soil conditions have on the site response (Seed et al., 1974) and to extend the results of Gutenberg (1957) about the effects of the local geologic conditions to the high frequency spectral amplitudes (Trifunac, 1976). Through the 1970's and early 1980's these studies were refined by detailed regression analyses which were made possible by the large number of well documented records of strong ground motion (Trifunac, 1976, 1979; Trifunac and Lee, 1988a,b,c). However, the above analyses considered either the local soil or the local geologic site conditions and never combined the simultaneous effects of both in the development of one and more general scaling relation .Since the typical dimensions of the local soil versus the local geologic site conditions are so different

it would be expected that their effects may be reflected in the recorded spectral amplitudes in high and in low frequencies respectively. If both of these effects can be shown to contribute significantly to the spectral amplitudes between 0.05 and 25 Hz, the frequency range of interest to earthquake engineering, then both soil and geologic site conditions should be considered simultaneously.

Trifunac(1987) presented detailed analysis of these effects and considered two different models for characterizing the local geologic conditions. One in terms of the overall depth of sediments to the basement rock, and the other in terms of the simple geological site classification (Trifunac and Brady, 1975). The latter approach to the characterization of the local geologic conditions is convenient when only surface geology maps are available. This is often the case particularly in preliminary analyses, before any detailed site investigations have been carried out. The aim of this paper is to summarize the results of Trifunac (1987) for this type of site characterization.

I: SCALING OF FOURIER SPECTRA IN TERMS OF M, R, H, S, h, s_L and v

I.1 The Current Model

Trifunac and Lee(1988b) presented a study which dealt with scaling of Fourier amplitude spectra, FS(T), in terms of magnitude, M, source-to-station distance R, focal depth, H, "size" of fault, S, component orientation, v and local geology, characterized by the local geological site parameter, s (or by the representative depth of sediments, h). Their scaling relation takes the form

$$\log_{10}FS(T)=M+\mathscr{A}tt(\Delta,\ M,\ T)+b_1(T)M+b_2(T)s+b_3(T)v+b_5(T)+b_6(T)M^2 \qquad (I.1.1)$$

They deleted the term $b_4(T)\Delta$ because it was found to be insignificant. Here $\mathscr{A}tt\ (\Delta,\ M,\ T)$ is the new frequency dependent attenuation function. It is of the form (Trifunac and Lee, 1988a):

$$\mathscr{A}tt\ (\Delta,\ M,\ T)=\begin{cases}\mathscr{A}_0(T)\log_{10}\Delta & R\leqslant R_0\\ \mathscr{A}_0(T)\log_{10}\Delta_0-(R-R_0)/200 & R>R_0\end{cases} \qquad (I.1.2)$$

with Δ, the representative source-to-station distance, given by

$$\Delta=S\ \ln\left[\frac{R^2+H^2+S^2}{R^2+H^2+S_0^2}\right]^{-\frac{1}{2}} \qquad (I.1.3)$$

and

$$\Delta_0=S\ \ln\left[\frac{R_0^2+H^2+S^2}{R_0^2+H^2+S_0^2}\right]^{-\frac{1}{2}} \qquad (I.1.4)$$

S_0 is the coherence radius of the source (Gusev, 1983). The term $\mathscr{A}_0(T)\log_{10}\Delta$ is used to calculate the attenuation function at distances R less than some transition distance R_0, where $\Delta=\Delta_0$. For distances $R>R_0$, the attenuation becomes a lin-

ear function of distance R with slope equal to -1/200. R_0 is (Trifunac and Lee, 1988a):

$$R_0=\frac{1}{2}\left(\frac{-200\mathscr{A}_0(T)(1-S_0^2/S^2)}{\ln 10}+\sqrt{\frac{200\mathscr{A}_0(T)(1-S_0^2/S^2)}{\ln 10}-4H^2}\right), \quad (I.1.5)$$

and is a function of H, S, S_0 and $\mathscr{A}_0$ (T). More detailed discussion of this attenuation function can be found in Trifunac and Lee (1988a).

Regression analysis using the above model, equation I.1.1, has been performed on the Fourier amplitude data FS (T) at 91 discrete periods T ranging from 0.04 to 15.0 sec. The data has been selected from 1314 components of data from 104 earthquakes in the western United States. A screening procedure was used to minimize the biases in the model that could result from uneven distribution of data among the different magnitudes (Trifunac and Lee, 1988b).

Replacing the Richter's empirical attenuation function (Richter, 1958) with the frequency dependent attenuation function mentioned above, has not only contributed the additional flexibility to estimating the Fourier spectral amplitudes, but also has decreased the residuals of actual data relative to the model predictions relative to our earlier regression models (Trifunac, 1976, 1979).

I.2 Updating the Database

The database of Trifunac and Lee(1988b) consisted of 438 free-field records with 3 components each, or a total of 1314 components from 104 earthquakes for the years from 1933 to 1983. The list of earthquakes contributing to the present data base has been updated to a total of 106, with addition of two recent events, the Coalinga Earthquake of 1983 and the Morgan Hill Earthquake of 1984, both in California. With the addition of 56 free-field records from these two events, the total number of free-field records is now 494, corresponding to 988 horizontal components and 494 vertical components, or a total of 1482 components.

To proceed with the present analysis, information on the soil site properties has been collected from various available sources, including different reports of the United States Geological Survey(U.S.G.S.), California Division of Mines and Geology (C.D.M.G.), Nuclear Regulatory Commission, University Reports and various consulting reports. At first this data has been characterized by a soil parameter, S_L, which was assigned values 1 for deep soil sites, 2 for stiff soil sites and 3 for "rock" sites (Seed, et al., 1976). Subsequently, this characterization was changed to 0 for "rock" sites, 1 for stiff soil sites and 2 for deep soil sites for convenience in regression analysis (Trifunac, 1987).

I.3 The New Scaling Relation

As pointed out in our previous analyses(Trifunac and Lee, 1985a), while the depth of sediments at each recording station represents a well defined quantitative

site characterization, in many instances, little may be known about such depth at some sites and so the scaling of FS (T) amplitudes there using depth, h, would be impossible. The qualitative geological site characterization in terms of s = 0 (sites on sediments), s = 1 (intermediate sites) and s = 2 (sites on basement rock (Trifunac and Brady, 1975)), thus remains a useful approach to the scaling of FS (T) amplitudes.

The previous scaling relation using geologic site characterization, s, is of the form (Trifunac and Lee, 1985a)

$$\log_{10}FS(T) = M_< + \mathscr{A}tt(\Delta, M, T) + b_1(T)M_{<>} + b_2(T)s + b_3(T)v + b_5(T) + b_6(T)M^2_{<>}, \quad (I.3.1)$$

where $M_<$ and $M_{<>}$ are defined in the following text. Here the variable for geological site characterization, s, has been treated as a quantitative variable in the scaling relation. To include the soil classification in the regression analysis, the regression equation of FS (T) to be used will now take the form:

$$\log_{10}FS(T) = M_< + \mathscr{A}tt(\Delta, M, T) + b_1(T)M_{<>} + b_2^{(1)}(T)S^{(1)} + b_2^{(2)}(T)S^{(2)} + b_3(T)v + b_4^{(1)}(T)S^{(1)}v + b_4^{(2)}(T)S^{(2)}v + b_5(T) + b_6(T)M^2_{<>} + b_7^{(1)}(T)S_L^{(1)} + b_7^{(2)}(T)S_L^{(2)}. \quad (I.3.2)$$

$S^{(1)}$ and $S^{(2)}$ represent a new pair of indicator variables for local geological site conditions:

$$S^{(1)} = \begin{cases} 1 & \text{if } s = 1, \\ 0 & \text{otherwise}, \end{cases}$$

and

$$S^{(2)} = \begin{cases} 1 & \text{if } s = 2, \\ 0 & \text{otherwise}, \end{cases} \quad (I.3.3a)$$

while $S_L^{(1)}$ and $S_L^{(2)}$ characterize the soil at the site where

$$S_L^{(1)} = \begin{cases} 1 & \text{if } S_L = 1, \\ 0 & \text{otherwise}, \end{cases}$$

and

$$S_L^{(2)} = \begin{cases} 1 & \text{if } S_L = 2, \\ 0 & \text{otherwise}, \end{cases} \quad (I.3.3b)$$

The use of the indicator variables $S^{(1)}$ and $S^{(2)}$ here instead of s, is due to the fact that s, is a qualitative variable which takes on the discrete values of 0, 1 and 2 for the three distinct types of geological site classifications (Trifunac and Brady 1975). The additional terms $b_4^{(i)}(T)S^{(i)}v$ together with $b_2^{(i)}(T)S^{(i)}$, for i = 1 and 2 will result in the coefficients characterizing the site condition, s, to be component dependent, so that for horizontal (v = 0) and vertical (v = 1) components, this takes the form (for i = 1, 2):

$$b_2^{(i)}(T)S^{(i)}+b_4^{(i)}(T)S^{(i)}v=\begin{cases}b_2^{(i)}(T)S^{(i)} & v=0\\ (b_2^{(i)}(T)+b_4^{(1)}(T))S^{(i)} & v=1\end{cases},$$

The scaling functions $b_1(T)$through $b_7^{(2)}(T)$have been determined through the regression analysis of the new database of 1482 components of spectral amplitudes, FS(T), at 91 discrete periods T ranging from 0.04 sec. to 15 sec. All procedures in data preparation, selection, and the procedures of the regression analysis employed here are identical to those described in more detail in Trifunac (1987). The computed coefficients at each period T resulting from linear regression are denoted by $\hat{b}_1(T)$ through $\hat{b}_7^{(2)}(T)$, respectively.

Substituting the fitted coefficients into equation (I.3.2) gives $\hat{FS}(T)$, the estimated spectral amplitudes, where

$$\begin{aligned}\log_{10}\hat{FS}(T)=&M+\mathscr{A}tt(\Delta,M,T)+\\&\hat{b}_1(T)M+\hat{b}_2^{(1)}(T)S^{(1)}+\hat{b}_2^{(2)}(T)S^{(2)}+\\&\hat{b}_3(T)v+\hat{b}_4^{(1)}(T)S^{(1)}v+\hat{b}_4^{(2)}(T)S^{(2)}v+\hat{b}_5(T)+\\&\hat{b}_6(T)M^2+\hat{b}_7^{(1)}(T)S_L^{(1)}+\hat{b}_7^{(2)}(T)S_L^{(2)}.\end{aligned}\qquad(I.3.4)$$

Equation (I.3.4) applies only in the range $M_{min}\leqslant M\leqslant M_{max}$, where for each periods, T:

$$\begin{aligned}&M_{min}(T)=-\hat{b}_1(T)/(2\hat{b}_6(T)),\text{ and}\\&M_{max}(T)=-(1+\hat{b}_1(T))/(2\hat{b}_6(T)),\end{aligned}\qquad(I.3.5)$$

and equation (I.3.4) is then modified to:

$$\begin{aligned}\log_{10}\hat{FS}(T)=&M_<+\mathscr{A}tt(\Delta,M,T)+\\&\hat{b}_1(T)M_{<>}+\hat{b}_2^{(1)}(T)S^{(1)}+\hat{b}_2^{(2)}(T)S^{(2)}+\\&\hat{b}_3(T)v+\hat{b}_4^{(1)}(T)S^{(1)}v+\hat{b}_4^{(2)}(T)S^{(2)}v+\hat{b}_5(T)+\\&\hat{b}_6(T)M_{<>}^2+\hat{b}_7^{(1)}(T)S_L^{(1)}+\hat{b}_7^{(2)}(T)S_L^{(2)},\end{aligned}\qquad(I.3.6)$$

with

$$M_<=\min(M,M_{max})$$

$$M_{<>}=\max(M_{min},M_<)=\begin{cases}M_{min} & M\leqslant M_{min}\\ M & M_{min}\leqslant M\leqslant M_{max}\\ M_{max} & M>M_{max}\end{cases}.$$

The residues $\varepsilon(T)=\log_{10}(FS(T))-\log_{10}(\hat{FS}(T))$ describing the distribution of the recorded FS(T) about the estimated $\hat{FS}(T)$ are next calculated. $\varepsilon(T)$ can be described by a normal distribution function with mean $\mu(T)$ and standard deviation $\sigma(T)$ (Trifunac, 1987),

$$p(\varepsilon,T)=\frac{1}{\sigma(T)\sqrt{2\pi}}\int_{-\infty}^{\varepsilon(T)}\exp\left[-\frac{1}{2}\left(\frac{x-\mu(T)}{\sigma(T)}\right)^2\right]dx \qquad (I.3.7)$$

where p (ε, T) is the probability that $\log_{10}[FS(T)]-\log_{10}[\hat{FS}(T)]\leqslant\varepsilon(T)$.

I.4 The Regression Coefficients

Figure I.4.1 shows the smoothed coefficients $\hat{b}_1(T)$, $\hat{b}_2^{(1)}(T)$, $\hat{b}_2^{(2)}(T)$, $\hat{b}_3(T)$, $\hat{b}_4^{(1)}(T)$, $\hat{b}_4^{(2)}(T)$, $\hat{b}_5(T)$, $\hat{b}_6(T)$, $\hat{b}_7^{(1)}(T)$ and $\hat{b}_7^{(2)}(T)$ (solid lines) together with the estimates of their 80%, 90% and 95% confidence intervals (dashed lines). Comparison of this figure with the corresponding figure I.5.1 in Trifunac (1987) for scaling in terms of h, the depth of sediments, shows that the scaling functions $\hat{b}_1(T)$, $\hat{b}_3(T)$, $\hat{b}_5(T)$, $\hat{b}_6(T)$, $\hat{b}_7^{(1)}(T)$ and $\hat{b}_7^{(2)}(T)$ in both figures are almost identical. These functions correspond to the same parameters, M, v, 1, M^2, $S_L^{(1)}$ and $S_L^{(2)}$, respectively, in the respective scaling relations. Their similarity thus demonstrates the consistency between the two scaling models. The functions $\hat{b}_2^{(1)}(T)$ and $\hat{b}_2^{(2)}(T)$, for $S^{(1)}$ (s = 1) and $S^{(2)}$ (s = 2), in Figure I.4.1 are both opposite in sign when compared to the corresponding function $b_2(T)$ for alluvial depth h in Figure I.5.1 in Trifunac (1987). This again shows consistency since s = 2 (for basement rock sites) corresponds to alluvial depth h = 0 km. Similar observation can be made for the functions $b_4^{(1)}(T)$ and $b_4^{(2)}(T)$ for $S^{(1)}v$ and $S^{(2)}v$, when compared with the corresponding function $b_4(T)$ for hv in Trifunac (1987).

Figure I.4.2 shows the plot of the residuals corresponding to the actual distribution of data relative to equation I.3.6 $p^*(\varepsilon, T) = 0.1$ through 0.9, for $\log_{10}$ FS(T). It is of interest to compare this figure with Figure I.5.2 in Trifunac (1987), since they both illustrate the spread of the observed data about their corresponding models, being different only in the method for characterization of the local site geology. As in our previous analyses (Trifunac and Lee, 1985a) the resemblance of the two figures demonstrates that with other factors being identical the uncertainties associated with the characterization of local geology in terms of the geological site conditions s = 0, 1 and 2, are not much greater than those associated with the site characterization in terms of the depth of sediments, h.

Figure I.4.3 shows the plot of the statistical parameters in the description of the distribution of residues (equation I.3.7), namely, $\hat{\mu}(T)$, $\hat{\sigma}(T)$, $x^2(T)$ and KS (T), from top to bottom. Note that in the entire period range from T = 0.04 sec. to T = 15 sec., both the X^2 and Kolmogorov-Smirnov, KS (T), tests fail to reject the hypothesis that the distribution is normal, with 95% confidence.

Table I.4.1 presents, for 12 periods, between T = 0.04 sec. and T = 14 sec., the

values of the smoothed regression coefficients $\hat{b}_1$ (T), $\hat{b}_2^{(1)}$ (T), $\hat{b}_2^{(2)}$ (T), $\hat{b}_3$ (T), $\hat{b}_4^{(1)}$ (T), $\hat{b}_4^{(2)}$ (T), $\hat{b}_5$ (T), $\hat{b}_6$ (T), $\hat{b}_7^{(1)}$ (T), $\hat{b}_7^{(2)}$ (T), M_{min} (T), M_{max} (T), the nine smoothed calculated residue levels corresponding to p* (ε, T) = 0.1 through 0.9, the smoothed coefficients $\hat{\mu}$ (T), $\hat{\sigma}$ (T) in equation (I.3.7), the χ^2 and the Kolmogorov-Smironov statistics. The 12 periods presented should be sufficient for most practical computations, especially since the smoothness of the coefficients is such that any interpolation scheme will yield adequate estimates of FS (T) in the entire period range from 0.04 sec. to 14 sec.

TABLE I.4.1

$$\log_{10}FS(T) = M_{\lhd} + \alpha tt(\Delta, M, T) + b_1(T)M_{\lhd\rhd} + b_2^{(1)}(T)S^{(1)} + b_2^{(2)}(T)S^{(2)} + b_3(T)v + b_4^{(1)}S^{(1)}v + b_4^{(2)}(T)S^{(2)}v + b_5(T) + b_6(T)M_{\lhd\rhd}^2 + b_7^{(1)}(T)S_L^{(1)} + b_7^{(2)}(T)S_L^{(2)}$$

MAG-SITE-SOIL DIRECT: 1-STEP MODEL

PERIOD, T (SEC)	.040	.065	.11	.19	.34	.50	.90	1.60	2.80	4.40	7.50	14.0
COEFFICIENTS:												
$b_1(T)$	.604	.629	.797	.971	1.039	1.017	.953	.990	1.138	1.140	.661	−.656
$b_2^{(1)}(T)$	−.161	−.138	−.100	−.077	−.101	−.141	−.193	−.191	−.138	−.082	−.025	.031
$b_2^{(2)}(T)$	−.092	−.86	−.070	−.086	−.145	−.183	−.207	−.205	−.225	−.251	−.245	−.157
$b_3(T)$	.140	.084	−.052	−.233	−.397	−.450	−.429	−.333	−.250	−.224	−.234	−.260
$b_4^{(1)}(T)$	.036	.039	.038	.042	.078	.124	.186	.173	.080	−.001	−.036	.021
$b_4^{(2)}(T)$	.021	.015	.006	.030	.102	.154	.206	.236	.270	.280	.211	−.002
$b_5(T)$	−3.686	−3.675	−4.009	−4.473	−4.853	−5.012	−5.237	−5.705	−6.291	−6.203	−4.464	−.049
$b_6(T)$	−.090	−094	−.110	−.127	−.134	−.130	−.120	−.119	−.129	−.133	−.103	−.011
$b_7^{(1)}(T)$	−.252	−.227	−.174	−.096	−.019	.026	.099	.178	.213	.180	.078	−.080
$b_7^{(2)}(T)$	−.183	−.187	−.174	−.117	−.027	.030	.113	.188	.218	.175	.034	−.209
M_{min}	3.367	3.351	3.615	3.815	3.891	3.906	3.968	4.168	4.411	4.295	3.220	.000
M_{max}	8.937	8.680	8.152	7.743	7.637	7.746	8.131	8.376	8.287	8.063	8.0881	4.500
RESIDUES:												
p = .1	−.590	−.566	−.514	−.455	−.417	−.416	−.443	−.474	−.482	−.469	−.442	−.417
p = .2	−.373	−.360	−.329	−.292	−.267	−.267	−.287	−.305	−.301	−.288	−.273	−.263
p = .3	−.230	−.219	−.199	−.175	−.162	−.163	−.179	−.190	−.184	−.170	−.154	−.143
p = .4	−.103	−.099	−.091	−.079	−.071	−.074	−.084	−.086	−.075	−.067	−.068	−.073
p = .5	.008	.006	.002	.000	.003	.006	.007	.011	.018	.020	.014	.007
p = .6	.126	.118	.103	.090	.085	.086	.092	.100	.107	.107	.099	.089
p = .7	.239	.228	.204	.180	.166	.168	.184	.201	.204	.195	.175	.157
p = .8	.369	.353	.323	.288	.266	.267	.287	.307	.307	.293	.271	.252
p = .9	.574	.549	.501	.444	.403	.398	.419	.442	.440	.422	.398	.376
RESIDUE STATISTICS:												
$\mu(T)$	.000	−.000	−.000	.000	.001	.000	−.000	.001	.004	.004	.002	−.001
$\sigma(T)$	.451	.432	.394	.348	.318	.317	.338	.360	.360	.346	.324	.306
$X^2(T)$	5.835	6.112	6.207	6.337	6.811	7.359	8.415	9.706	10.795	10.921	10.105	9.457
KS(T)	.029	.031	.031	.031	.031	.031	.032	.036	.042	.046	.047	.047

I . 5 Examples of Estimated Fourier Spectra

Figure I .5.1 presents four sets of plots of estimated FS (T) spectra using equation (I . 3 . 6) . The top two sets are examples of FS(T)computed for magnitudes M = 4.5, 5.5, 6.5 and 7.5 at epicentral distance R = 0, focal depth H = 5 km, for soil parameter s_L = 1 (stiff soil), for p(ε, T) = 0.5 and for the horizontal and vertical motions. The solid lines in both figures correspond to the geologic site condition s = 2 (basement rock), while the dashed lines correspond to s = 0 (sediments). The diagonal dashed lines represent the average Fourier amplitudes of digitization and processing noise. The lower left plot illustrates the effect of epicentral distance R on the changes of spectral amplitudes for magnitudes M = 6.5, focal depth H = 5 km, geologic site condition s = 0 , soil classification s_L = 1, p(ε, T) = 0.5 and for horizontal(solid lines)and vertical(dashed lines)components. Four sets of curves corresponding to R = 0, 25, 50 and 100 km are presented. The lower right plot illustrates the effect of focal depth H on the change of spectral amplitudes.

Figure I .5. 2 presents another four plots of estimates FS (T) to illustrate the effects of local soil conditions on FS(T). It is observed that for periods up to 0.3 sec., the spectral amplitudes FS(T) at "rock" sites (s_L = 0) are higher than those at deep soil sites(s_L = 2). Beyond ~0.3 sec., this trend is reversed up to the periods of about 10 sec.,so that within this intermediate period range the Fourier amplitudes at deep soil sites are slightly higher than those at the rock sites.

Figures I . 5 . 3 and I . 5 . 4 compare the differences of the effects the local geologic and local soil site characteristics have on FS(T).Figure I . 5 . 3 .consists of three plots,one for each local soil classification(s_L = 0, 1 and 2).For each plot, the FS(T)has been computed for the local geological site condition s = 0,1 and 2. This figure shows that for all local soil site classifications, in the whole period range considered, the Fourier amplitudes increase for the sites on sediments (s = 0).Figure 1.5.4 also shows three plots, one for each geological site classification (s = 0, 1 and 2). For each s, the soil classification ranges from s_L = 0("rock")to 1(stiff soil) and to 2(deep soil). It is seen that for periods up to ~0.3 sec. the Fourier amplitudes, FS(T), on s_L = 0("rock") sites are higher than those with s_L = 1(stiff soil), or s_L = 2(deep soil). Beyond ~0.3 sec., this trend is reversed up to periods of about 10 sec. The two figures (I .5.3 and I .5.4) show that local geological and local soil parameters have different characteristics at different period ranges and that both are significant but in a different way.

Figures I .5.5 through I .5.7 present examples of how the horizontal and vertical Fourier amplitudes computed from equation (1.3.6) compare with the actual Fourier spectra for the corresponding components of recorded strong-motion data at various sites. The agreement between the actual and estimated FS (T) amplitudes is

good.

Ⅱ.1 The Residue Two Step Model

The previous sections in this paper dealt with the direct, "1-step" model where the scaling of Fourier spectra in terms of M,R, H,S,s,s_L and v has been performed in one step, with the soil indicator variables included in the regression equation directly. Here we consider another alternative in which the regression model which doesn't include soil classification may have already been developed and the scaling functions $\hat{b}_1(T)$through $\hat{b}_6(T)$ estimated. The first step of this procedure is to scale the Fourier spectra in terms of all the parameters except for soil site classification:

$$\log_{10}\hat{FS}(T)=M_{<}+\mathscr{A}tt(\Delta,M,T)+\hat{b}_1(T)M_{<>}+\hat{b}_2^{(1)}(T)S^{(1)}+\hat{b}_2^{(2)}(T)S^{(2)}+\hat{b}_3(T)v+\hat{b}_4^{(1)}(T)S^{(1)}v+\hat{b}_4^{(2)}(T)S^{(T)}v+\hat{b}_5(T)+\hat{b}_6(T)M^2_{<>}. \quad (Ⅱ.1.1)$$

The residues, $\varepsilon(T)=\log_{10}FS(T)-\log_{10}\hat{FS}(T)$,at each site where soil classification is available are then fitted by the equation

$$\varepsilon(T)=b_7^{(1)}(T)S_L^{(1)}+b_7^{(2)}(T)S_L^{(2)}+b_8(T). \quad (Ⅱ.1.2)$$

Combining equation(Ⅱ.1.1 and Ⅱ.1.2)gives

$$\log_{10}\hat{FS}(T)=M_{<}+\mathscr{A}tt(\Delta,\ M,\ T)+\hat{c}_1(T)M_{<>}+\hat{c}_2^{(1)}(T)S^{(1)}+\hat{c}_2^{(2)}(T)S^{(2)}+\hat{c}_5(T)+\hat{c}_6(T)M^2_{<>}+c_7^{(1)}(T)S_L^{(1)}+c_7^{(2)}(T)S_L^{(2)}, \quad (Ⅱ.1.3)$$

where $\hat{c}_i(T)=\hat{b}_i(T)$, except for $\hat{c}_5(T)$, with

$$\hat{c}_5(T)=\hat{b}_5(T)+\hat{b}_8(T) \quad (Ⅱ.1.4)$$

This procedure can be called" 2 -step"model in contrast with the direct"1-step"model presented earlier. Detailed comparison of the corresponding results of the direct" 1 -step"model and this "2-step"model shows a lot of similarity between the two analyses (Trifunac, 1987). The shapes of the scaling functions are very similar, the residues for the nine probability levels have almost identical widths, and the estimated FS amplitudes are also very similar. One advantage that the residue " 2 -step" model has over the direct " 1 -step" model is that in the" 2 -step"model, the first step of regression (equation(Ⅱ.1.1)) can be performed on a larger database including sites where information on soil classification is absent. It is only in the second step (equation(Ⅱ.1.2)) that regression has to be performed on that part of the database for the sites with available soil classification.Thus as more information on soil site classification becomes available, only the second step of iteration needs to be repeated to update the scaling functions. As for the direct"1-step"model,the regres-

sion analysis can be performed only on that part of the database for sites with soil classification. Every time this part of the database is updated, the whole regression has to be repeated.

DISCUSSION AND CONCLUSION

The forms of the empirical equations we used are not new, but have evolved, from our previous work (Trifunac 1976, 1979; Trifunac and Lee, 1988b, c). The idea, which has been introduced here for the first time, is to use the local soil and the local geologic characteristics of the site simultaneously in the development of the regression models. Also, the term sv, reflecting the directional dependence of the amplification has not been employed in our previous analyses. We found that the proposed model fits the data well and that there is consistency among different regression models (Trifunac, 1987). No significant differences in the overall residual amplitudes have been observed between 1-step and 2-step regression models. Relative to our previous studies, the amplitudes of the residuals we found in this investigation are smaller.

To enable qualitative comparison of the results with some earlier investigations, which employed the local site characterization in terms of the local soil classification only, Trifunac (1987) carried out such analyses as well, by ignoring the local geologic features of the sites. Since the functional form of the dependence of the spectral amplitudes on the geological site classification is similar to its dependence on the local soil conditions,he found that ignoring the local geologic conditions may lead to exagerated amplitude factors "representing" the local soil conditions. We conclude that both the local soil and the local geologic site conditions must be used together in the selection of the site specific Fourier amplitude spectra.

ACKNOWLEDGEMENTS

This work was initiated at the Dept. of Civil Engineering, University of Southern California. It was completed at the School of Civil Engineering, Kyoto University, with generous support of the Japan Society for Promotion of Science.

REFERENCES

Duke, M.(1958). Effects of Ground on Destructiveness of Large Earthquakes,Proc. ASCE, 84, No.SM3.

Gusev, A.A.(1983). Descriptive Statistical Model of Earthquake Source Radiation

and Its Application to an Estimation of Short Period Strong Motion, Geoph.J. R.Astr.Soc. **74**, 787—808.

Gutenberg, B. (1957). Effects of Ground on Earthquake Motion,Bull. Seism. Soc. Amer., **47**, 221—520.

Haskell, N.(1960). Crustal Reflection of Plane SH Waves, J.Geoph.Res.,**65**, 4147—4150.

Kanai, K. (1949, 1951). Relation Between the Earthquake Damage of Non-Wooden Buildings and the Nature of the Ground, Bull. Earthquake Res. Inst.,Vol.27, p. 97(1979); Vol.29, p. 209(1951).

Lee, V.W. and M. D. Trifunac(1985). Attenuation of Modified Mercalli Intensity for Small Epicentral Distance in California, Dept. of Civil Eng. Report No. CE 85—01, Univ. Southern Calif. Los Angeles, California.

Lee, V.W. and M. D. Trifunac (1987). Strong Earthquake Ground Motion Data in EQINFOS; Part 1, Dept. of Civil Eng. Report No. CE 87—01, Univ. of Southern Calif., Los Angeles, California.

Medvedev, S.V.(1955). Ocenka Seizmicheskoi balnoski u zavisimosti ot gruntovih uslovi, Tr.Geofiz.Inst.AN SSSR No.4(141).

Montgomery and Peek (1982). Introduction to Linear Regression Analysis, J.Wiley and Sons, 1982.

Richter, C.F.(1958). Elementary Seismology, Freeman and Co., San Francisco.

Seed, H.B., C. Ugas and J.Lysmer(1974). Site Dependent Spectra for Earthquake Resistant Design,E.E.R.C. 74—12, U.C.Berkeley.

Seed, H.B., C. Ugas and J. Lysmer(1976).Site Dependent Spectra for Earthquake Resistant Design, Bull. Seism. Soc. Amer., **66**, 221—243.

Trifunac, M. D. (1971). Surface Motion of Semi-Cylindrical Alluvial Valley for Incident Plane SH Waves, Bull. Seism. Soc.Amer., **61**, 1755—1770.

Trifunac, M.D.(1976). Preliminary Empirical Model for Scaling Fourier Amplitude Spectra of Strong Ground Acceleration in Terms of Earthquake Magnitude, Source to Station Distance and Recording Site Conditions, Bull. Seism. Soc. Amer., **66**, 1343—1373.

Trifunac,M.D.(1979). Preliminary Empirical Model for Scaling Fourier Amplitude Spectra of Strong Motion Acceleration in Terms of Modified Mercalli Intensity and Geologic Site Conditions, Int. J. Earthquake Eng. and Structural Dynamics, **7**,63—74.

Trifunac, M. D. and A.G. Brady (1975). On the Correlation of Seismic Intensity Scales with the Peaks of Recorded Strong Ground Motion, Bull. Seism. Soc. Amer., **65**, 139—162

Trifunac, M.D.and V.W. Lee (1985a). Preliminary Empirical Model for Scaling

Fourier Amplitude Spectra of Strong Ground Acceleration in Terms of Earthquake Magnitude, Source to Station Distance, Site Intensity and Recording Site Conditions, Dept.of Civil Eng.Report No.CE 85-05, Univ.Southern Calif., Los Angels, California.

Trifunac, M.D. and V.W. Lee (1985b). Preliminary Empirical Model for Scaling Pseudo Relative Velocity Spectra of Strong Earthquake Accelerations in Terms of Magnitude, Distance, Site Intensity and Recording Site Conditions, Dept. of Civil Eng. Report No. CE 85—04, Univ. Southern Calif.,Los Angeles,California.

Trifunac, M.D. (1987).Influence of Local Soil and Geologic Site Conditions on Fourier Spectrum Amplitudes of Recorded Strong Motion Accelerations, Dept. of Civil Eng. Report No. CE 87-04, Univ. of Southern California, Los Angels, California.

Trifunac, M.D. And V.W. Lee (1988a). Frequency Dependent Attenuation of Strong Earthquake Ground Motion, Int. J. Soil Dynamics and Earthquake Eng. (in press).

Trifunac, M.D. and V.W. Lee (1988b).Empirical Models for Scaling Fourier Amplitude Spectra of Strong Ground Acceleration in Terms of Earthquake Magnitude, Source to Station Distance, Site Intensity and Recording Site Conditions, Int. J.Soil Dynamics and Earthquake Eng.(in press).

Trifunac, M.D. and V.W. Lee (1988c). Empirical Models for Scaling Pseudo Relative Velocity Spectra of Strong Earthquake Accelerations in Terms of Magnitude, Distance, Site Intensity and Recording Site Conditions, Int. J. of Soil Dynamics and Earthquake Eng. (in press).

Tsai, N.C.(1969). Influence of Local Geology on Earthquake Ground Motion, EERL,Calif. Inst. of Tech., Pasadena.

Zhou, Xi-Yuan(1965). Effect of Soil Classification on Structural Damage During Strong Motion Earthquakes, Earthquake Eng. Research Report Vol Ⅱ, 27—43, Institute of Engineering Mechanics, Academia Sinica, Harbin, China.

FIGURE CAPTIONS

Figure Ⅰ.4.1. Functions $b_1^{(2)}(T)$ through $b_7^{(2)}(T)$ (full lines) in equation Ⅰ.3.6 and the estimates of their 80, 90 and 95 percent confidence intervals (dashed lines).

Figure Ⅰ.4.2. Distribution of residuals (irregular full lines and smooth full lines) relative to the scaling model Ⅰ.3.6. Smooth dashed lines represent analytical approximation $p(\varepsilon,T)$to the observed residuals.

Figure Ⅰ.4.3. $\hat{\mu}(T)$ and $\hat{\sigma}(T)$, average and standard deviation (full lines) used in

description of p(ε,T)and their 95 percent confidence intervals(top two diagrams) Actual (full lines) and permissible (dashed lines), with 95 percent confidence, amplitudes of $X^2(T)$ and Kolmogorov- Smirnov, KS (T) tests are shown in bottom two diagrams.

Figure I .5.1 Top: Estimated Fourier Amplitude spectra (inches/sec)for p(ε, T) = 0.5, M = 4.5, 5.5, 6.5 and 7.5, basement rock sites (s = 2) (full lines) and alluvium (s = 0) (dashed lines), for focal depth H = 5km, stiff soil sites ($s_L = 1$), Zero epicentral distance (R = 0 km) and for horizontal (left) and vertical (right)motions.

Bottom: Estimated Fourier Amplitude Spectra (inches/sec), for p(ε, T) = 0.5, M = 6.5, alluvium site(s = 0), horizontal(full lines)and vertical (dashed lines) motions, and for stiff soil sites ($s_1 = 1$).Left: Focal depth H = 5 km and epicentral distance R = 0, 25, 50 and 100km. Right: Epicentral distance R = 0 km and focal depth H = 5, 10, 25 and 50km

Figure I .5.2. Top:Estimated Fourier Amplitude Spectra (inches/sec)for p(ε, T) = 0.5, M = 4.5, 5.5, 6.5 and 7.5, site on sediments(s = 0),epicentral distance R = 0km, focal depth H = 5km, for "rock" sites ($s_L = 0$) (full lines) and deep soil sites($s_L = 2$)(dashed lines).

Bottom: Estimated Fourier Amplitude spectra (inches/sec) for p(ε, T) = 0.5, M = 6.5, epicentral distances R = 0, 25, 50 and 100km, focal depth H = 5km, site on sediments (s = 0), "rock" sites($s_L = 0$)(full lines)and deep soil site ($s_L = 2$) (dashed lines), for horizontal (left)and vertical (right) motions.

Figure I .5.3. Estimated Fourier Amplitude spectra, p(ε, T) = 0.5, M = 6.5, source depth H = 5km, epicentral distance R = 25km, horizontal motions, sites on sediments(s = 0) (short dashed lines), intermediate sites (s = 1)(dashed lines) and basement rock sites (s = 2), and on "rock" sites ($s_L = 0$)(left), stiff soil sites ($s_L = 1$)(center) and deep soil sites($s_L = 2$)(right).

Figure I .5.4, Estimated Fourier Amplitude spectra, p (ε, T) = 0.5, for M = 6.5, source depth H = 5km,epicentral distance R = 25km, horizontal motions,on"rock" sites($s_L = 0$)(full lines), stiff soil sites ($s_L = 1$) (long dashed lines) and deep soil sites ($s_L = 2$)(short dashed lines), for basement rock sites(s = 2)(left), intermediate sites(s = 1)(center)and sites on sediments(s = 0)(right),

Figure I .5.5. Comparison of actual(AG106, CALTECH SEISMOLOGICAL LAB. 1971, M = 6.5, R = 36.1km, H = 13km, s = 2 and $s_L = 0$) and estimated Fourier spectrum amplitudes for p(ε,T) = 0.1, 0.5 and 0.9 and for horizontal (left)and vertical (right)motions.

Figure I .5.6 Comparison of actual(AB021 VERNON CMD BLDG 1933, M = 6.3,

R = 47.8km, H = 16km, s = 0, s_L = 1) and estimated Fourier Spectrum amplitudes for p(ε, T) = 0.1, 0.5 and 0.9 and for horizontal (left) and vertical (right) motions.

Figure I.5.7. Comparison of actual(AA001 EL CENTRO, 1940, M = 6.4, R = 9.3 km, H = 5km, s = 0, s_L = 2) and estimated Fourier Spectrum Amplitudes for p (ε,T) = 0.1, 0.5 and 0.9 and for horizontal(left)and vertical(right)motion.

记录到的强震加速度的傅氏幅值谱基于震级与局部土质、地质条件的经验标定

M. D. Trifunac

(美国南加州大学)

提 要

本文提供了强震加速度傅氏幅值谱的新的标定方程，用来表征基于土质和地质场地分类参数的局部场地条件。文中表明，土质与地质场地条件两者应同时应用于场地特定幅值谱的估计。

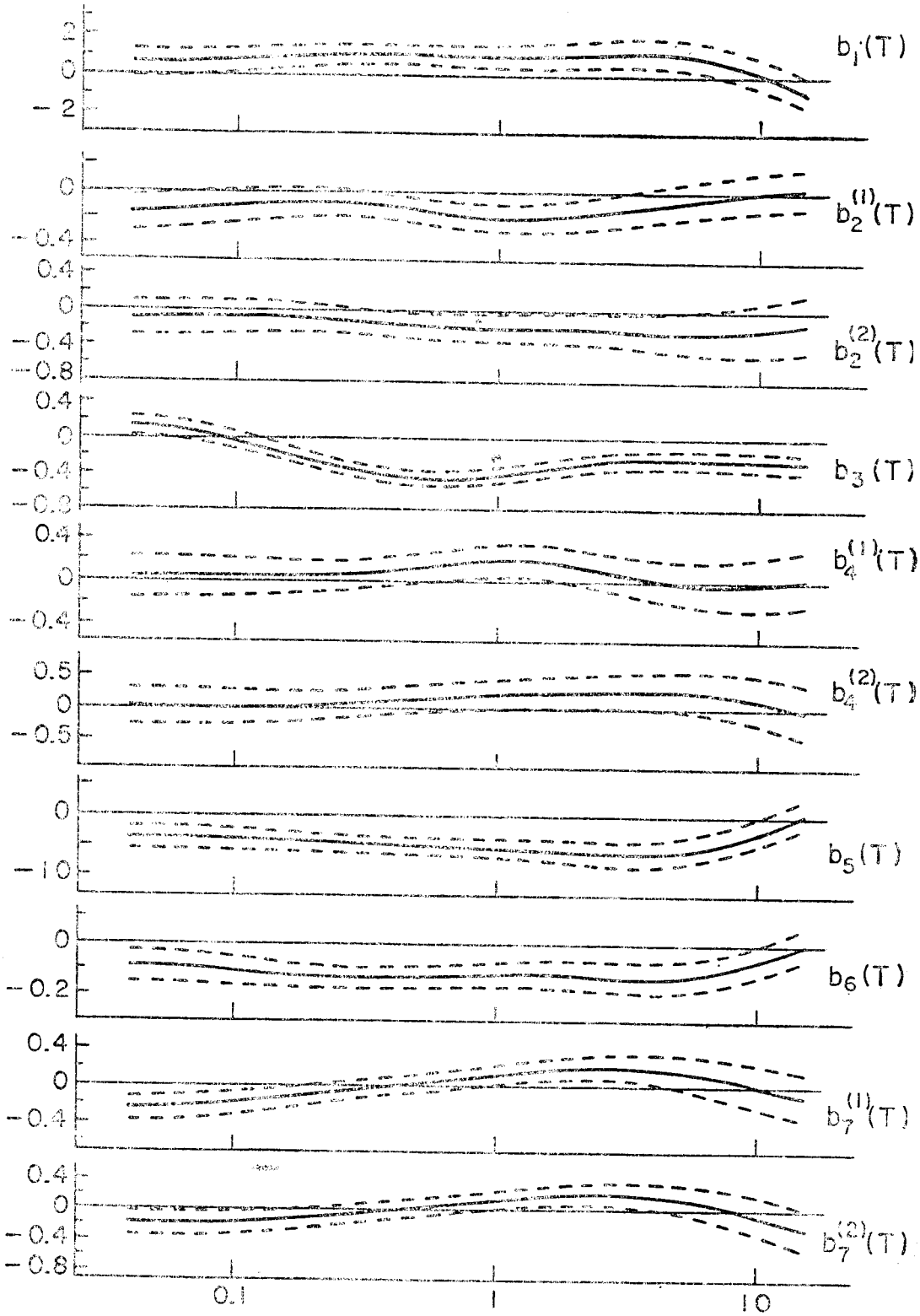
2
0
−2
$b_1(T)$
0
−0.4
$b_2^{(1)}(T)$
0.4
0
−0.4
−0.8
$b_2^{(2)}(T)$
0.4
0
−0.4
−0.8
$b_3(T)$
0.4
0
−0.4
$b_4^{(1)}(T)$
0.5
0
−0.5
$b_4^{(2)}(T)$
0
−10
$b_5(T)$
0
−0.2
$b_6(T)$
0.4
0
−0.4
$b_7^{(1)}(T)$
0.4
0
−0.4
−0.8
$b_7^{(2)}(T)$
0.1
1
10
PERIOD, sec

Figure I. 1

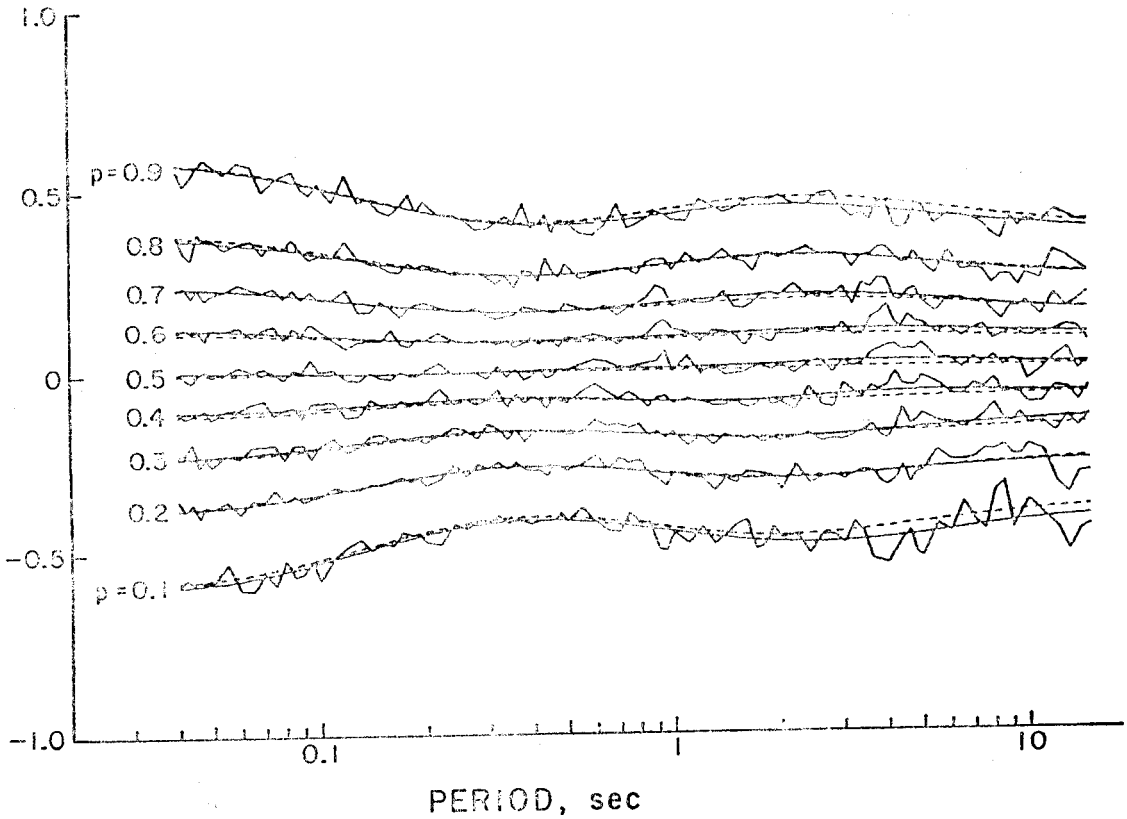

Figure I.4.2

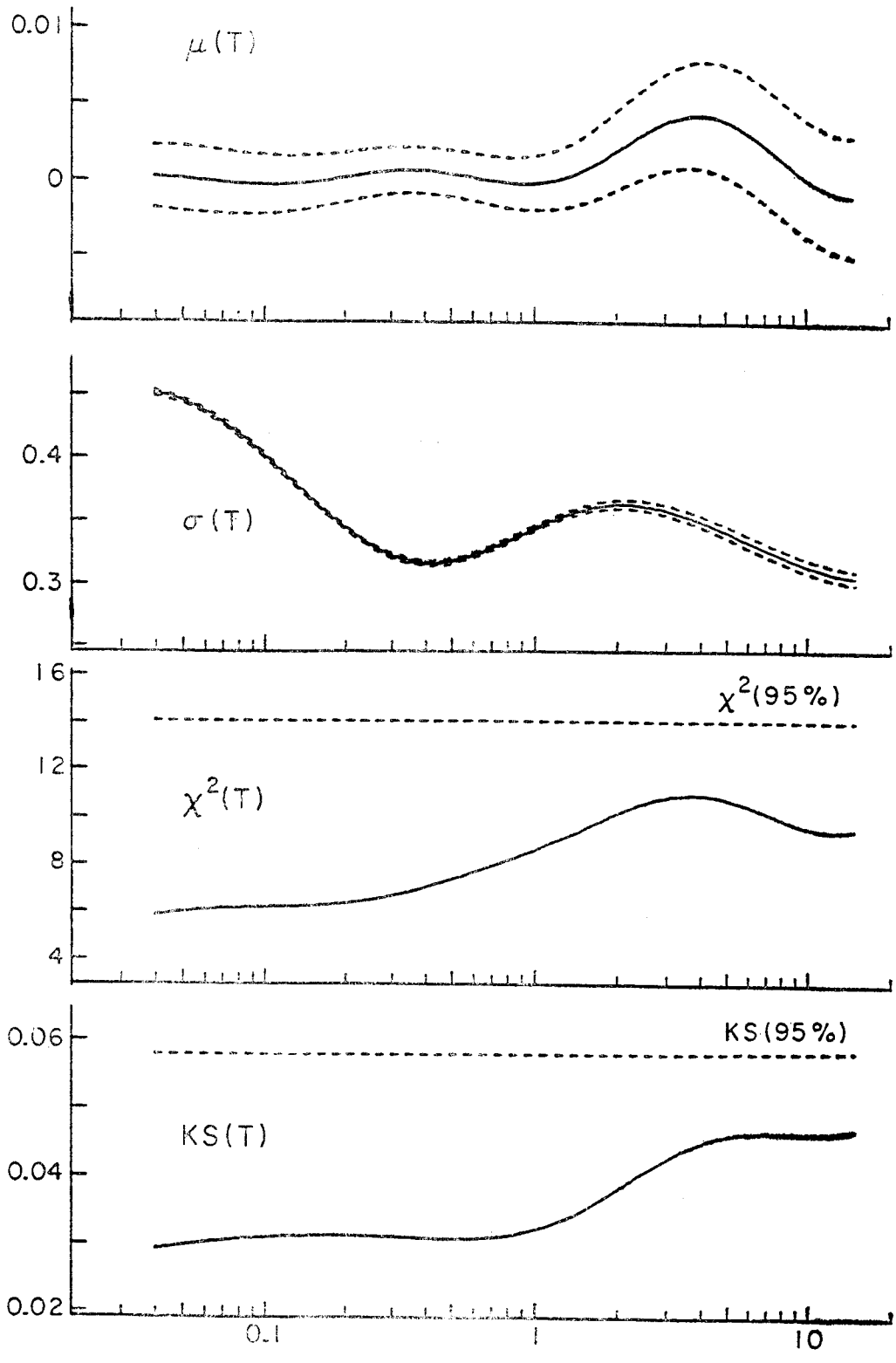
0.01
μ(T)
0
0.4
σ(T)
0.3
16
χ²(95%)
12
χ²(T)
8
4
0.06
KS(95%)
KS(T)
0.04
0.02
0.1
1
10
PERIOD, sec

Figure I.4.3

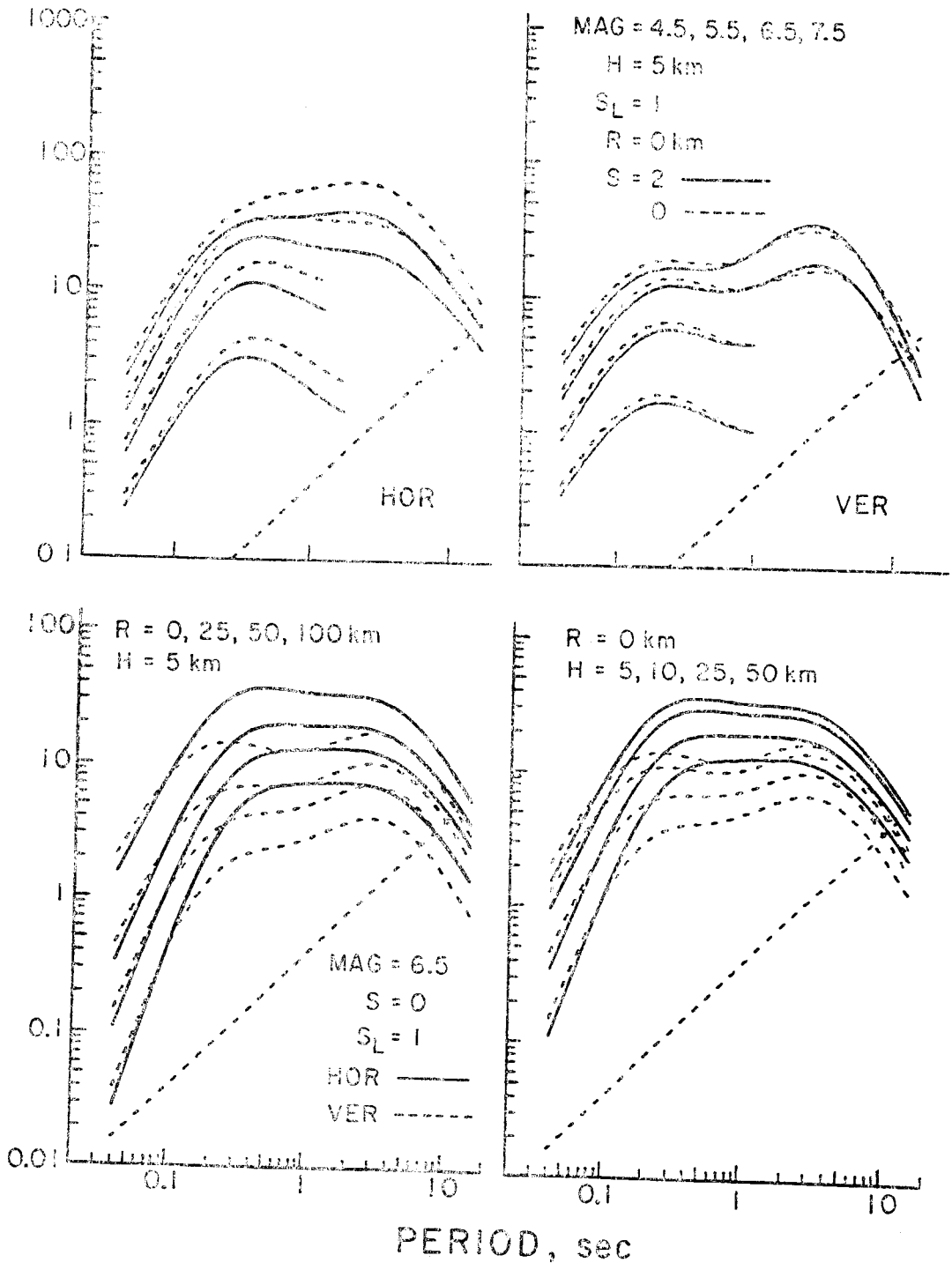
1000
100
10
1
0.1
HOR
MAG = 4.5, 5.5, 6.5, 7.5
H = 5 km
S_L = 1
R = 0 km
S = 2
0
VER
100
10
1
0.1
0.01
R = 0, 25, 50, 100 km
H = 5 km
MAG = 6.5
S = 0
S_L = 1
HOR
VER
R = 0 km
H = 5, 10, 25, 50 km
0.1
1
10
PERIOD, sec

Figure I.5.1

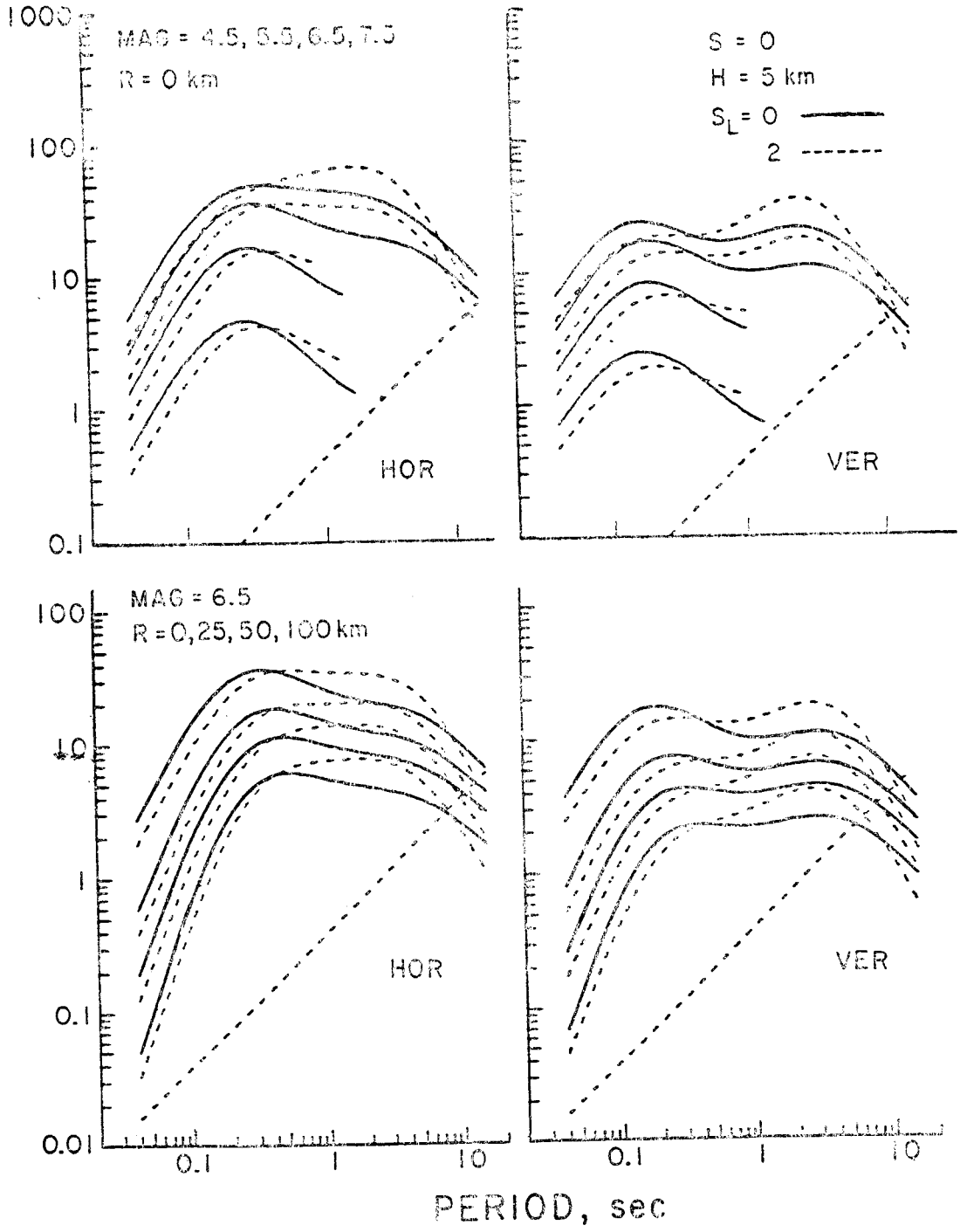
MAG = 4.5, 5.5, 6.5, 7.5
R = 0 km
S = 0
H = 5 km
S_L = 0
2
HOR
VER
MAG = 6.5
R = 0, 25, 50, 100 km
HOR
VER
1000
100
10
1
0.1
0.01
0.1
1
10
PERIOD, sec

Figure I.5.2

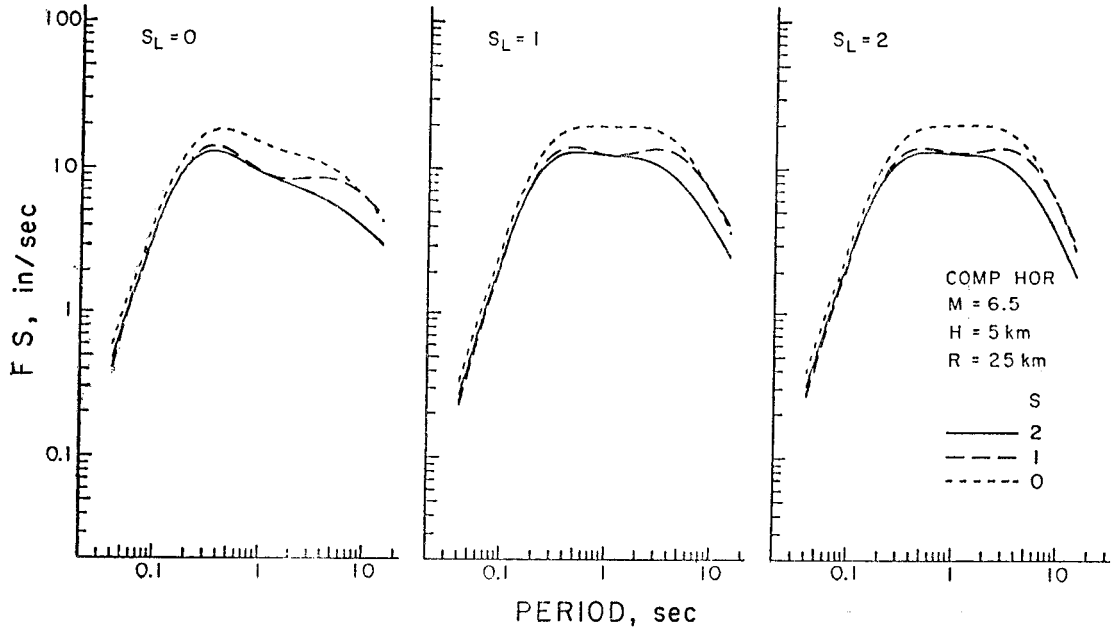
100
10
1
0.1
FS, in/sec
SL = 0
SL = 1
SL = 2
0.1
1
10
PERIOD, sec
COMP HOR
M = 6.5
H = 5 km
R = 25 km
S
2
1
0

Figure I.5.3

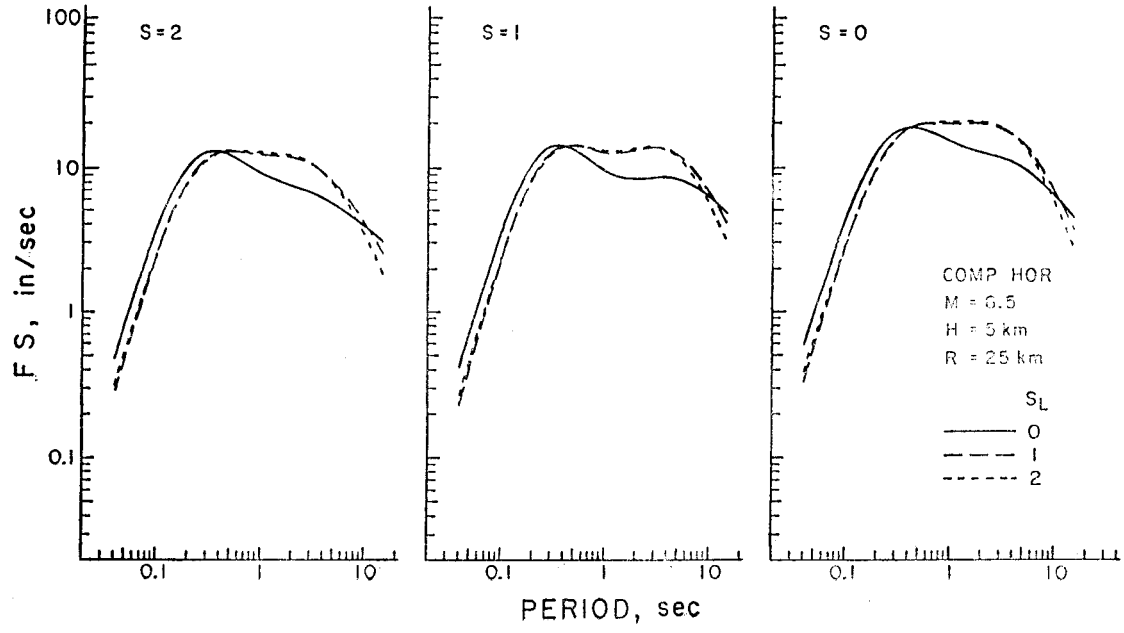

Figure I.5.4

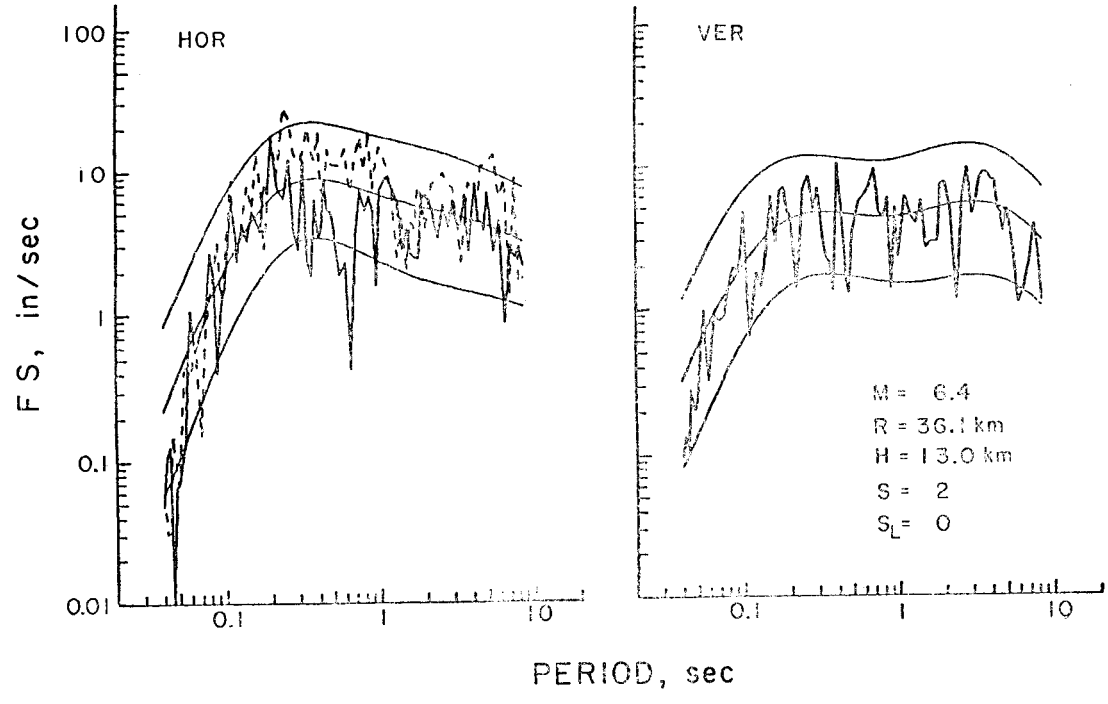

Figure I.5.5

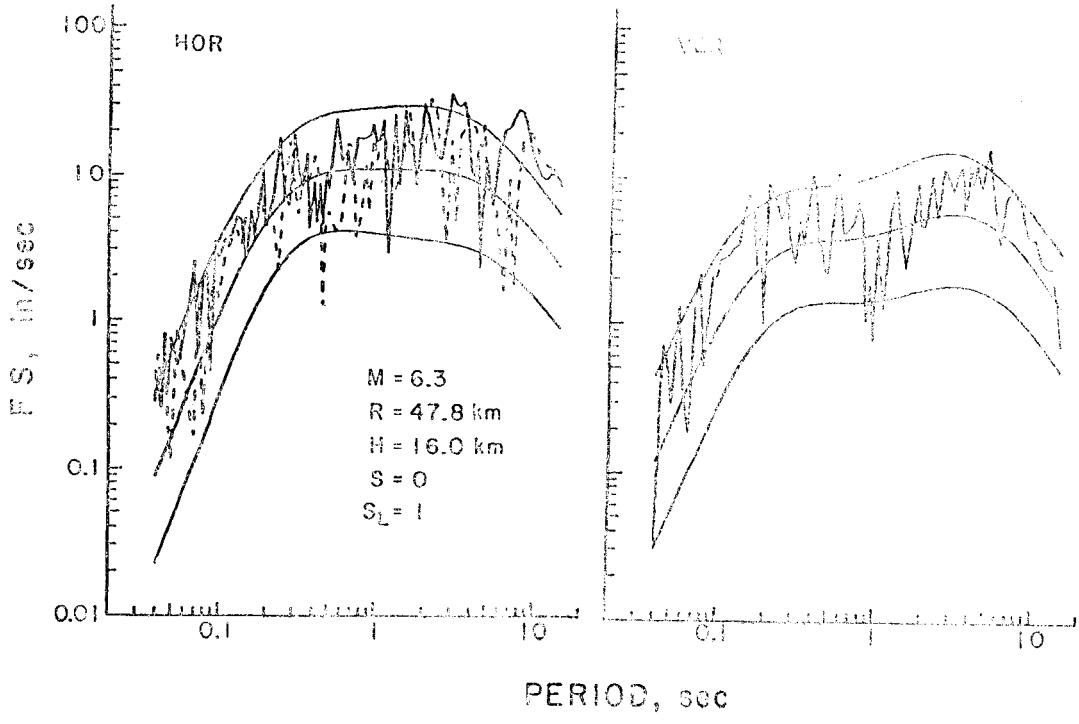

Figure I.5.6

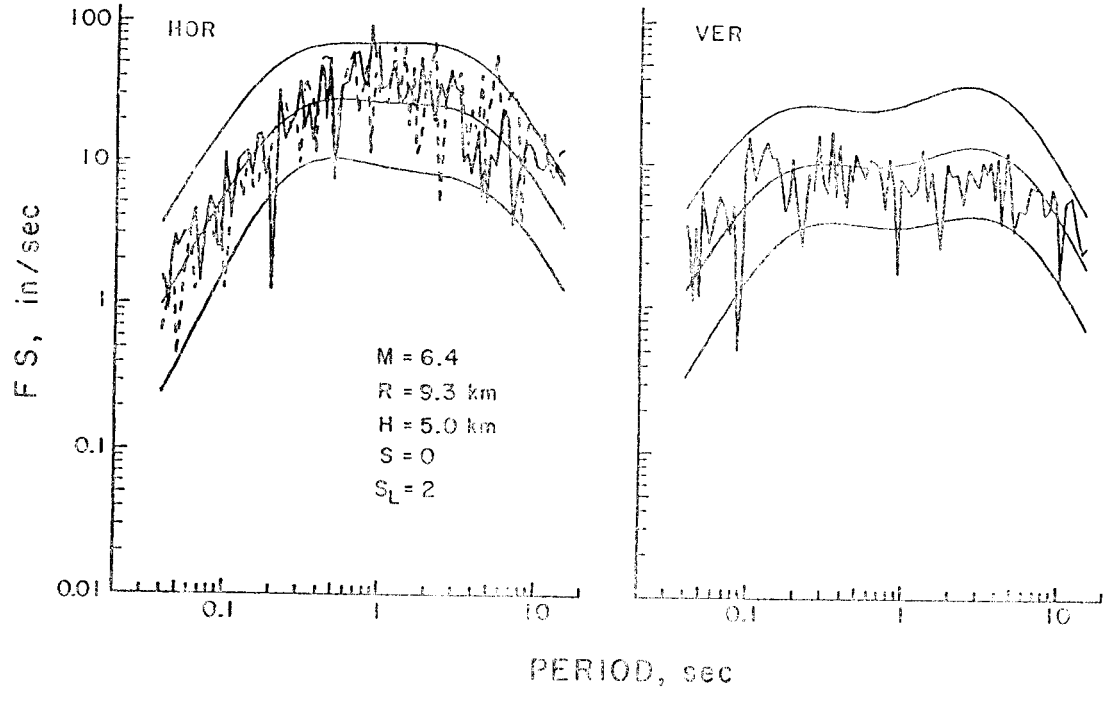

Figure I.5.7